VERSITA
ADVANCES IN MANUFACTURING SCIENCE AND TECHNOLOGY Vol. 37, No. 2, 2013
DOI: 10.2478/amst-2013-0012

ESTIMATION OF CUTTING FORCE MODEL COEFFICIENTS WITH REGULARIZED INVERSE PROBLEM

Piotr Pawełko, Bartosz Powałka, Stefan Berczyński

Summary

In this paper, a method for estimation of cutting force model coefficients is proposed. The method makes use of regularized total least squares to identify the cutting forces from the measured acceleration signals and the frequency response function (FRF) matrix. An original regularization method is proposed which is based on the relationship between the harmonic components of the cutting forces. Numerical tests are performed to evaluate the effectiveness of the method. The method is compared with unregularized methods and common Tikhonov regularization combined with GCV and L-curve methods. It was found that the proposed method provides more accurate estimates of the cutting force coefficcients than the unregularized method and common regularization techniques. Furthermore the influence of acceleration measurement errors, FRF matrix errors and FRF matrix conditioning on the accuracy of the estimated coefficients is investigated. It was concluded that FRF matrix errors influence the most the accuracy of the results.

Keywords: force identification, acceleration, FRF matrix, regularization, cutting force model

Estymacja współczynników modelu siły skrawania z zastosowaniem technik regularyzacji

Streszczenie

W artykule zaproponowano metodę estymacji współczynników modelu siły skrawania. Metoda stosuje regularyzowaną technikę ortogonalnych najmniejszych kwadratów dla identyfikacji sił skrawania na podstawie mierzonych sygnałów przyśpieszeń oraz macierzy częstotliwościowych funkcji przejścia. Zaproponowano oryginalną metodę regularyzacji opartą na zależności pomiędzy składnikami harmonicznymi sił skrawania. Przeprowadzono symulację numeryczną weryfikującą skuteczność metody. Przedstawiona metoda jest porównana z podejściem bez regularyzacji oraz regularyzowanym metodą Tikhonova stosowaną wraz z metodami GCV oraz L-curve. Pozwala uzyskać dokładniejsze oszacowanie wartości współczynników niż estymacja bez regularyzacji lub z regularyzacją Tikhonova. Dokonano również oceny wpływu błędu pomiaru przyśpieszeń, błędów macierzy funkcji przejścia oraz jej uwarunkowania na dokładność estymowanych współczynników. Na podstawie przeprowadzonej analizy wykazano, że największy wpływ mają błędy macierzy funkcji przejścia.

Słowa kluczowe: identyfikacja siły, przyspieszenia, macierzy częstotliwościowych funkcji przejścia, regularyzacja, model siły skrawania

Address: Prof. Stefan BERCZYŃSKI, Piotr PAWEŁKO, Ph.D. Eng., Bartosz POWAŁKA, D.Sc. Eng., Department of Mechanical Engineering and Mechatronics, West Pomeranian University of Technology Szczecin, Piastów 19, 70-310 Szczecin, e-mails: Piotr.Pawelko@zut.edu.pl, Bartosz.Powalka@zut.edu.pl

1. Introduction

The measurement of cutting forces is required to estimate the cutting force model coefficients. The coefficients of the mechanistic force model are frequently used to produce stability lobes diagrams that provide cutting parameters that ensure stable machining. Such cutting coefficients are very often determined directly from the milling tests for the specific material-cutting tool pair. During the cutting test the cutting forces are measured by a force dynamometer and then the coefficients of the force model are estimated to fit the analytically expressed forces to the experimental ones [1-5]. Such an approach is recommended in research laboratories but it is not favored in industrial practice for numerous reasons. For instance, usage of a dynamometer in an industrial plant during production is troublesome. This is due to the fact that mounting a dynamometer requires changes to a fixture as well as modification of the NC code. This leads to not only production disruption but also increases costs.

This paper presents a method for estimating cutting force model coefficcients using acceleration signals that can be easily measured without disrupting the production process. Cutting forces can be estimated by using the experimentally measured frequency response function and applying inverse identification techniques [6].

The cutting forces model is presented in Section 2 and the FRF matrix construction is shown in Section 3. The time domain representation of cutting forces is transformed into frequency domain and harmonic components of cutting forces are used to derive the regularization matrix in Section 4. Section 5 describes the numerical experiment. The objective of the numerical studies was to compare the proposed regularization method with unregularized solutions and common regularization techniques. Addditionally, the influence of various factors on the solution i.e. acceleration measurement error, impact force measurement error, conditioning of the FRF matix and error of the FRF matrix were investigated. It was found that the proposed approach provides an accurate estimation of coefficients that relate cutting forces with the chip cross-sectional area.

2. Force model

Mechanistic cutting force models assume that cutting forces are proportional to the chip cross-sectional area. The constants that relate to such cutting forces and the chip cross-sectional area are called specific cutting force coefficients. They depend on cutter geometry, inserts and piece materials as well as cutting conditions. Mechanistic cutting force models often incorporate the effect of the cutting edge which is proportional to the depth of cut. The constants of proportionality are referred to as edge constants. Then the tangential, F_{ci},

radial, F_{ti} and axial, F_{ai} cutting forces acting on the ith cutting edge (Fig. 1) are functions of instantaneous chip thickness $f_z \sin(\varphi_i)$ and depth of cut a_p:

$$\left.\begin{aligned} F_{ci}(t) &= \left(K_c a_p f_z \sin\left(\phi_i(t)\right) + K_{ce} a_p\right) h_i\left(\phi_i(t)\right) \\ F_{ti}(t) &= \left(K_t a_p f_z \sin\left(\phi_i(t)\right) + K_{te} a_p\right) h_i\left(\phi_i(t)\right) \\ F_{ai}(t) &= \left(K_a a_p f_z \sin\left(\phi_i(t)\right) + K_{ae} a_p\right) h_i\left(\phi_i(t)\right) \end{aligned}\right\} \quad h_i\left(\phi_i(t)\right) = \begin{cases} 1 \; if \; \phi_i(t) \in (\phi_{enter}; \phi_{exit}) \\ 0 \; if \; \phi_i(t) \notin (\phi_{enter}; \phi_{exit}) \end{cases} \tag{1}$$

where: f_z is feed per tooth (mm) and φ_i is instantaneous angular location of the i^{th} cutting edge, t is time, the coefficients K_c, K_t and K_a are the specific cutting force coefficients in tangential, radial and radial directions respectively. The coefficients K_{ce}, K_{te} and K_{ae} are the edge constants, the φ_{enter} and φ_{exit} are immersion angles at entry and exit state.

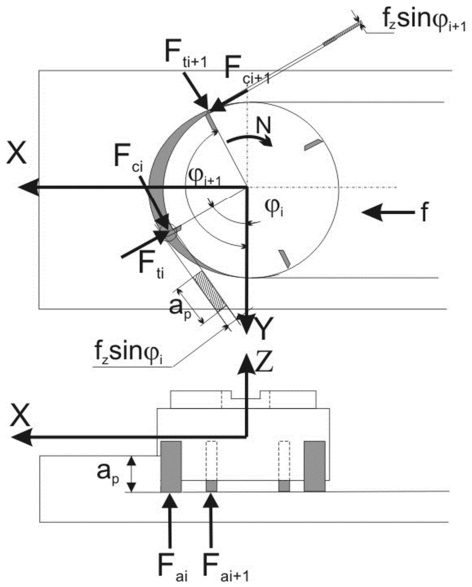

Fig. 1. Geometry of the end milling process

Local cutting forces from the working cutting edges expressed by formula (1) can be easily transformed into feed $\mathbf{F}_x$, cross-feed $\mathbf{F}_y$ and axial $\mathbf{F}_z$ global forces (Fig. 1). For a cutter with *z* cutting edges it takes the following form:

$$\mathbf{F}(t)=\sum_{i=1}^{z}\begin{bmatrix}-\cos(\phi_i(t)) & -\sin(\phi_i(t)) & 0\\ \sin(\phi_i(t)) & -\cos(\phi_i(t)) & 0\\ 0 & 0 & 1\end{bmatrix}\begin{bmatrix}F_{ci}(t)\\ F_{ti}(t)\\ F_{ai}(t)\end{bmatrix} \tag{2}$$

where $\mathbf{F}(t)=\begin{bmatrix}\mathbf{F}_x(t) & \mathbf{F}_y(t) & \mathbf{F}_z(t)\end{bmatrix}^T$

Global cutting forces (2) can be expressed as a function of cutting coefficients:

$$\mathbf{F}(t)=\mathbf{W}(t)\mathbf{K} \tag{3}$$

Where $\mathbf{K}=\begin{bmatrix}K_c & K_{ce} & K_t & K_{te} & K_a & K_{ae}\end{bmatrix}$ and

$$\mathbf{W}(t)=\sum_{i=1}^{z}h_i(t)a_p\begin{bmatrix}-f_t\sin(\varphi_i)\cos(\varphi_i) & -\cos(\varphi_i) & -f_t\sin^2(\varphi_i) & -\sin(\varphi_i) & 0 & 0\\ f_t\sin^2(\varphi_i) & \sin(\varphi_i) & -f_t\sin(\varphi_i)\cos(\varphi_i) & -\cos(\varphi_i) & 0 & 0\\ 0 & 0 & 0 & 0 & f_t\sin(\varphi_i) & 1\end{bmatrix} \tag{4}$$

Cutting forces $\mathbf{F}(t)$ can be transformed into a frequency domain by applying Fourier transform to equation (3):

$$\mathbf{F}(\omega)=\mathbf{W}(\omega)\mathbf{K} \tag{5}$$

Since $\mathbf{W}(t)$ is a periodic function that results from the periodic pulse functions $h_i(t)$. Its Fourier transform is represented by the spectral lines spaced along the frequency axis at intervals $\omega_t=2\pi/\tau$. The time period τ depends on spindle speed N [RPM] and number of cutting edges *z*, $\tau=60/(Nz)$. Thus the k^{th} harmonic component of the cutting force vector is

$$\mathbf{F}(k\omega_t)=\mathbf{W}(k\omega_t)\mathbf{K} \tag{6}$$

Frequently the Z-direction is much stiffer than X and Y and therefore it does not significantly influence the stability of the milling process. In such cases, cutting force model coefficients K_a and K_{ae} are not required. Then the matrices $\mathbf{W}(t)$ and $\mathbf{W}(\omega)$ are reduced to the first two rows and the first four columns, e.g.:

$$\begin{bmatrix} F_x(t) \\ F_y(t) \end{bmatrix} = \left\{ \sum_{i=1}^{z} h_i a_p \begin{bmatrix} -f_t \sin(\varphi_i)\cos(\varphi_i) & -\cos(\varphi_i) & -f_t \sin^2(\varphi_i) & -\sin(\varphi_i) \\ f_t \sin^2(\varphi_i) & \sin(\varphi_i) & -f_t \sin(\varphi_i)\cos(\varphi_i) & -\cos(\varphi_i) \end{bmatrix} \right\} \begin{bmatrix} K_c \\ K_{ce} \\ K_t \\ K_{te} \end{bmatrix} \tag{7}$$

The reduced $\mathbf{W}(t)$ and $\mathbf{W}(\omega)$ matrics will be referred to as $\mathbf{W}_r(t)$ and $\mathbf{W}_r(\omega)$ respectively.

3. Frequency response function matrix

The frequency response function (FRF) is defined as the ratio between the harmonic response of the system and the harmonic force. For the purpose of stability analysis, the system response is expressed in the form of displacements [7]. The FRF matrix that is used for generating stability lobes relates the cutting forces to the relative tool-workpiece displacements. Very often, for convenience, the FRF matrix used in stability analysis is obtained by performing an impact hammer test on the cutting tool and workpiece. The instrumented hammer exerts a force in the directions of the cutting forces and an accelerometer is used to measure the response of the system at the cutting tool and the workpiece.

Owing to the fact that it is impossible to mount the accelerometer on the tool during cutting, the FRF matrix used for the purpose of force reconstruction must be measured at different locations. Moreover, contrary to the FRF matrix being used for stability analysis, it can be used for force identification and can have any form including accelerance relating measured accelerations signals (Fig. 2) $\mathbf{a}(\omega) = \left[a_1(\omega) \quad a_2(\omega) \quad \ldots \quad a_L(\omega) \right]^T$ to the applied force $\mathbf{F}(\omega) = \left[F_x(\omega) \quad F_y(\omega) \quad F_z(\omega) \right]^T$ as:

$$\mathbf{a}(\omega) = \mathbf{G}(\omega)\mathbf{F}(\omega) \tag{8}$$

When L accelerometers are used for force reconstruction the FRF matrix has a form:

$$\mathbf{G}(\omega)=\begin{bmatrix} G_{1x}(\omega) & G_{1y}(\omega) & G_{1z}(\omega) \\ G_{2x}(\omega) & G_{2y}(\omega) & G_{2z}(\omega) \\ \vdots & \vdots & \vdots \\ G_{Lx}(\omega) & G_{Ly}(\omega) & G_{Lz}(\omega) \end{bmatrix} \tag{9}$$

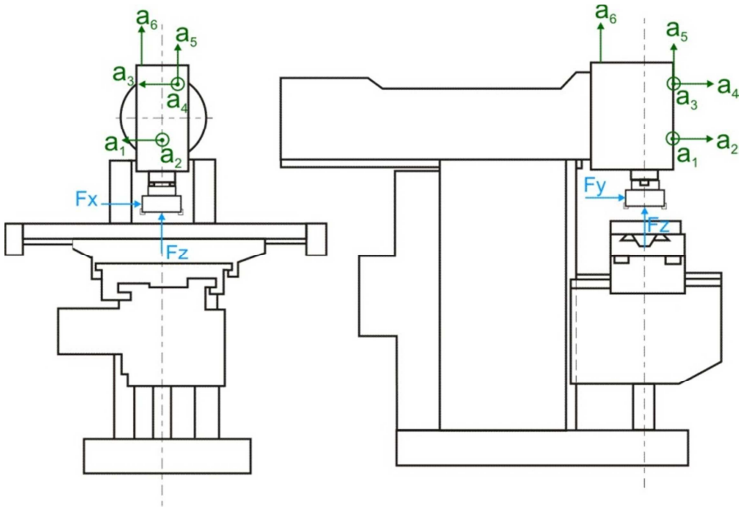

Fig. 2. Sample location of the sensors used in cutting force reconstruction

4. Cutting force reconstruction

4.1. Identification of the cutting force

The forces generated in the cutting process act on the machine structure causing vibrations. The accelerations measured by L accelerometers are related to the cutting forces in the frequency domain through the FRF matrix (9). Due to the fact that the frequency representation of the cutting forces during a stable cut is dominated by the tooth passing frequency, $\omega_t = z2\pi N/60$ and its harmonics the response of the structure will be also dominated by these components. Fourier coefficients of the measured accelerations at the k^{th} harmonic of the tooth passing frequency are:

$$\mathbf{a}(k\omega_t)=\mathbf{G}(k\omega_t)\mathbf{F}(k\omega_t) \tag{10}$$

Identification of the cutting force is limited to the 2 first harmonics (k = 1, 2) the following matrix equation can be written:

$$\underbrace{\begin{bmatrix}\mathbf{a}(\omega_t)\\ \mathbf{a}(2\omega_t)\end{bmatrix}}_{\mathbf{a}^{1-2}}=\underbrace{\begin{bmatrix}\mathbf{G}(\omega_t) & 0\\ 0 & \mathbf{G}(2\omega_t)\end{bmatrix}}_{\mathbf{G}^{1-2}}\underbrace{\begin{bmatrix}\mathbf{F}(\omega_t)\\ \mathbf{F}(2\omega_t)\end{bmatrix}}_{\mathbf{F}^{1-2}} \tag{11}$$

Thus, Fourier coefficients of the cutting forces can be estimated by means of least squares (LS). LS approach consists in minimizing:

$$\min_{F^{1-2}}\left\|\mathbf{G}^{1-2}\mathbf{F}^{1-2}-\mathbf{a}^{1-2}\right\|_2^2 \tag{12}$$

LS assumes that only the acceleration signal is charged with errors. In order to solve more general problems, where the FRF matrix also suffers from errors, the total least square (TLS) can be applied. Its application is theoretically justified because the frequency response function is usually determined by means of impact tests and therefore, the errors in the force and acceleration measurements influence its estimate. TLS minimizes a sum of weighted squared residuals:

$$\min_{F^{1-2}}\frac{\left\|\mathbf{G}^{1-2}\mathbf{F}^{1-2}-\mathbf{a}^{1-2}\right\|_2^2}{\left\|\mathbf{F}^{1-2}\right\|_2^2+1} \tag{13}$$

LS and TLS might not provide a good solution when FRF matrix $\mathbf{G}^{1-2}$ is nearly rank-deficient or it is highly affected by noise. Additionally errors present in the acceleration signal may lead to meaningless force harmonics estimates. Regularization may be applied in order to stabilize the solution. Frequently Tikhonov regularization is applied. It consists in minimizing $\left\|\mathbf{G}^{1-2}\right\|$:

$$\min_{F^{1-2}}\left\|\mathbf{G}^{1-2}\mathbf{F}^{1-2}-\mathbf{a}^{1-2}\right\|_2^2+\lambda^2\left\|\mathbf{F}^{1-2}\right\|_2^2 \tag{14}$$

Regularization parameter λ is found in the present research using generalized cross-validation [8] and L-curve methods [9].

The proposed regularization consists in imposing a constraint on the solution vector. When equality constrains are applied the formulations of regularized least squares and regularized total least squares are as follows:

$$\min_{F^{1-2}}\left\|\mathbf{G}^{1-2}\mathbf{F}^{1-2}-\mathbf{a}^{1-2}\right\|_2^2 \quad subject\,to \quad \left\|\mathbf{L}\mathbf{F}^{1-2}\right\|_2^2=\delta^2 \tag{15}$$

$$\min_{F^{1-2}} \frac{\left\| \mathbf{G}^{1-2}\mathbf{F}^{1-2} - \mathbf{a}^{1-2} \right\|_2^2}{\left\| \mathbf{F}^{1-2} \right\|_2^2 + 1} \quad subject\ to \quad \left\| \mathbf{L}\mathbf{F}^{1-2} \right\|_2^2 = \delta^2 \tag{16}$$

4.2. Regularization matrix

Regularization matrix L is chosen to obtain a solution with desirable properties. In the present paper, derivation of the regularization matrix L consists in finding the relationship between the first and second harmonic components of the cutting forces. It can be concluded from the matrix $\mathbf{W}$ (4) that only F_x and F_y components are related via coefficients K_c, K_{ce}, K_t and K_{te}.

Usually the stability analysis is performed in X-Y plane because of the high stifnness in the axial direction In such a case only K_c and K_t coefficients are required to model cutting forces. In order to estimate these coefficients feed and cross-feed cutting forces must be measured. Applying trigonometric formulas to (7) cutting forces can be expressed as:

$$\begin{aligned} F_x = & -\frac{1}{2}K_t a_p f_z \sum_{i=1}^{z} h_i \\ & + \frac{1}{2}K_t a_p f_z \sum_{i=1}^{z} \cos\left(2\left(\phi + \frac{i-1}{z}2\pi\right)\right) h_i - K_{te} a_p \sum_{i=1}^{z} \sin\left(\phi + \frac{i-1}{z}2\pi\right) h_i \\ & - \frac{1}{2}K_c a_p f_z \sum_{i=1}^{z} \sin\left(2\left(\phi + \frac{i-1}{z}2\pi\right)\right) h_i - K_{ce} a_p \sum_{i=1}^{z} \cos\left(\phi + \frac{i-1}{z}2\pi\right) h_i \end{aligned} \tag{17}$$

$$\begin{aligned} F_y = & \frac{1}{2}K_c a_p f_z \sum_{i=1}^{z} h_i \\ & - \frac{1}{2}K_c a_p f_z \sum_{i=1}^{z} \cos\left(2\left(\phi + \frac{i-1}{z}2\pi\right)\right) h_i + K_{ce} a_p \sum_{i=1}^{z} \sin\left(\phi + \frac{i-1}{z}2\pi\right) h_i \\ & - \frac{1}{2}K_t a_p f_z \sum_{i=1}^{z} \sin\left(2\left(\phi + \frac{i-1}{z}2\pi\right)\right) h_i - K_{te} a_p \sum_{i=1}^{z} \cos\left(\phi + \frac{i-1}{z}2\pi\right) h_i \end{aligned} \tag{18}$$

where $\phi = (2\pi N/60)t$ is the angular location of the leading cutting edge (i = 1).

Fourier transforms of these terms due to the periodical nature have non-zero values only at harmonics of the tooth passing frequency. When applying the

basic properties of the Fourier transform the 1st and 2nd harmonics of the particular terms are:

$$\left.\begin{aligned}
F_x(\omega_t) &= \left(-K_c a_p f_z \frac{30}{N} - \frac{8}{3\pi} K_{ce} a_p \frac{30}{N}\right) + j\left(K_t a_p f_z \frac{30}{N} + \frac{16}{3\pi} K_{te} a_p \frac{30}{N}\right) \\
F_y(\omega_t) &= \left(K_t a_p f_z \frac{30}{N} + \frac{8}{3\pi} K_{te} a_p \frac{30}{N}\right) + j\left(K_c a_p f_z \frac{30}{N} + \frac{16}{3\pi} K_{ce} a_p \frac{30}{N}\right) \\
F_x(2\omega_t) &= -\frac{4}{15\pi} K_{ce} a_p \frac{30}{N} + j\frac{16}{15\pi} K_{te} a_p \frac{30}{N} \\
F_y(2\omega_t) &= \frac{4}{15\pi} K_{te} a_p \frac{30}{N} + j\frac{16}{15\pi} K_{ce} a_p \frac{30}{N}
\end{aligned}\right\} \quad (19)$$

Performing simple operations, we have:

$$jF_x(\omega_t) + F_y(\omega_t) - j\frac{5}{3}F_x(2\omega_t) - \frac{5}{3}F_y(2\omega_t) = 0 \quad (20)$$

Thus the regularization matrix L for the searched vector $\left[F_x(\omega_t) \quad F_y(\omega_t) \quad F_z(\omega_t) \quad F_x(2\omega_t) \quad F_y(2\omega_t) \quad F_z(2\omega_t)\right]^T$ is:

$$\mathbf{L} = \left[\begin{array}{cccccc} j & 1 & 0 & -j\frac{5}{3} & -\frac{5}{3} & 0 \end{array}\right] \quad (21)$$

Matrix L imposes the equality constraint:

$$\mathbf{L}\mathbf{F}^{1-2} = 0 \quad (22)$$

4.3. Estimation of cutting force model coefficients

Matrix L is used to determine cutting force vector $\mathbf{F}^{1-2}$ from (16). The obtained cutting force vector harmonic components are then used to calculate the cutting force model coefficients $(K_c, K_{ce}, K_t, K_{te})$ utilizing formula (6) for the reduced matrix $\mathbf{W}_r(k\omega_t)$. The following equation is obtained when one separates real and imaginary parts and takes into consideration the first and second harmonic of tooth passsing frequency:

$$\begin{bmatrix} \mathrm{Re}\left(F_x\left(\omega_t\right)\right) \\ \mathrm{Re}\left(F_y\left(\omega_t\right)\right) \\ \mathrm{Im}\left(F_x\left(\omega_t\right)\right) \\ \mathrm{Im}\left(F_y\left(\omega_t\right)\right) \\ \mathrm{Re}\left(F_x\left(2\omega_t\right)\right) \\ \mathrm{Re}\left(F_y\left(2\omega_t\right)\right) \\ \mathrm{Im}\left(F_x\left(2\omega_t\right)\right) \\ \mathrm{Im}\left(F_y\left(2\omega_t\right)\right) \end{bmatrix} = \begin{bmatrix} \mathrm{Re}\left(\mathbf{W}_r\left(\omega_t\right)\right) \\ \mathrm{Im}\left(\mathbf{W}_r\left(\omega_t\right)\right) \\ \mathrm{Im}\left(\mathbf{W}_r\left(2\omega_t\right)\right) \\ \mathrm{Re}\left(\mathbf{W}_r\left(2\omega_t\right)\right) \end{bmatrix} \begin{bmatrix} K_c \\ K_{ce} \\ K_t \\ K_{te} \end{bmatrix} \tag{23}$$

This equation is used to determine values of cutting force model coefficients using LS method.

5. Numerical experiment

The aim of the numerical experiment was to compare the accuracy of the estimated cutting coefficients obtained based on the cutting forces identified with the method of least squares, the orthogonal method of least squares, the regularized method of orthoganal least squares and Tikhonov regularization combined with GCV and L-curve methods. The factors influencing the errors of the estimated cutting coefficients might include experimental inaccuracies of the determined FRF matrix as well as inaccuracies of the acceleration signal measurement performed during machine cutting. Errors of the frequency response functions determined in an impulse test result from the measurement errors of the exciting force and the response registered in the form of an acceleration signal. The conditioning of the transfer matrix $\mathbf{G}^{1-2}\left(\omega\right)$ may well be an additional factor possibly influencing the error of the estimates. Owing to the fact that the conditioning of the FRF matrix depends on frequency, the cutting forces were generated for various spindle rotational speeds. The FRF matrix used in the numerical experiment was modelled with the use of 3 modes of vibrations with natural frequencies of 60, 82 and 103 Hz and corresponding modal damping of 0.1, 0.15 and 0.07. It was assumed that 6 acceleration signals as shown in Fig. 1 would be used for the identification. Thus, the FRF matrix $\mathbf{G}^{1-2}\left(\omega\right)$ has the size of 12x6.

The FRF matrix was determined for the assumed system based on a simulated impulse test, where both the force loading the system and the registered acceleration were burdened with the Gaussian error. The frequency response functions were estimated by means of H1 estimator based on 9 averages. The FRF matrix with errors was used for force reconstruction. Figure 3 presents comparison of the precise FRF with the function determined in the simulated impulse test. In this test standard deviations in force and acceleration measurement were set to 5 N and 0.4 m/s^2 respectively.

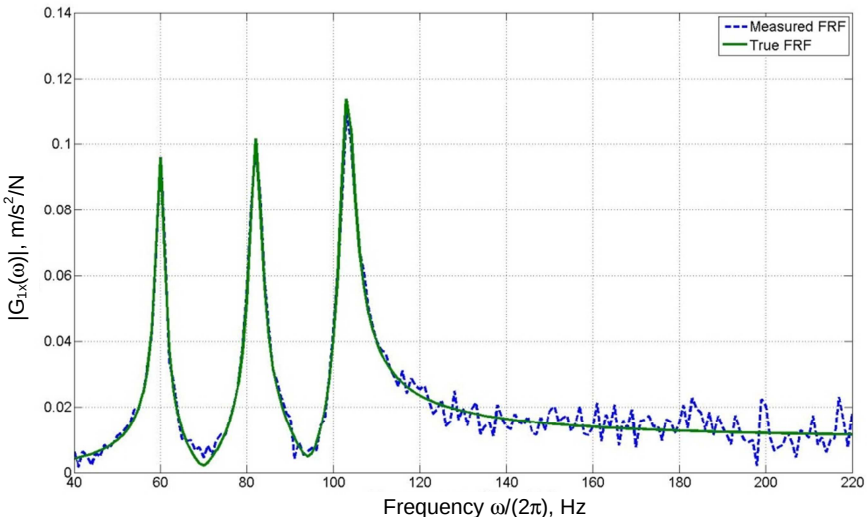

Fig. 3. Amplitude of the "true" and "measured" frequency response function G1x(w)

The machine tool structure was excited by cutting forces corrseponding to a full immersion cutting with a 2-blade cutter. The cutting forces were determined using formula (2) with the assumption of the following values of the specific cutting force coefficients of $K_{tc} = 1000$ N/mm^2, $K_{rc} = 700$ N/mm^2 and $K_{ac} = 250$ N/mm^2 as well as the edge constants of $K_{te} = 50$ N/mm, $K_{re} = 30$ N/mm and $K_{ae} = 15$ N/mm at depth of cut $a_p = 2$ mm, feed per tooth $f_z = 0.15$ mm. These parameters were kept constant throughout the tests and the spindle speed was varied to obtain different tooth passing frequencies.

The acceleration signals were determined based on the simulated (exact – Fig. 4) cutting forces and the precise value of the FRF matrix. The acceleration signals determined in this way were burdened with errors in the same way as was the case in the impulse test simulation. An example of the acceleration

signal with the assumed random error with standard deviation $\sigma = 0.4$ m/s^2 is presented in Fig. 5.

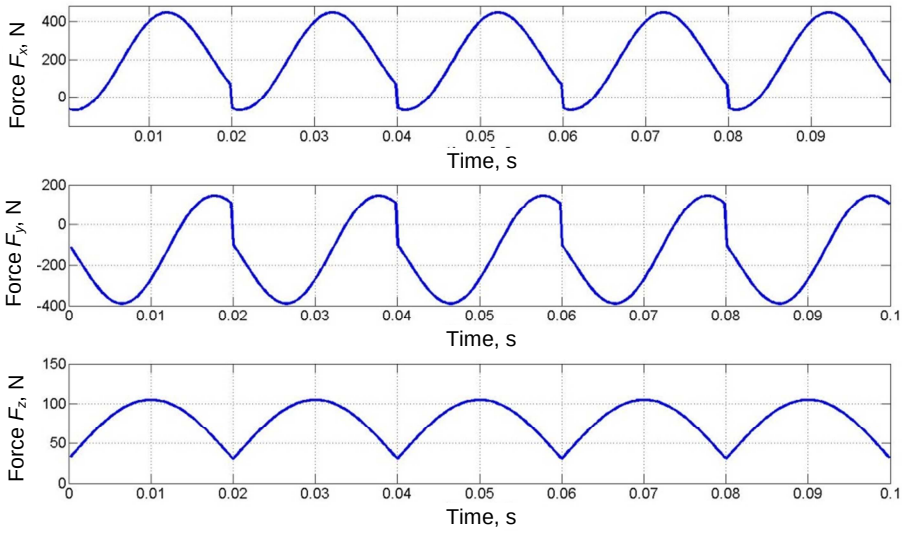

Fig. 4. Cutting forces exciting the investigated structure

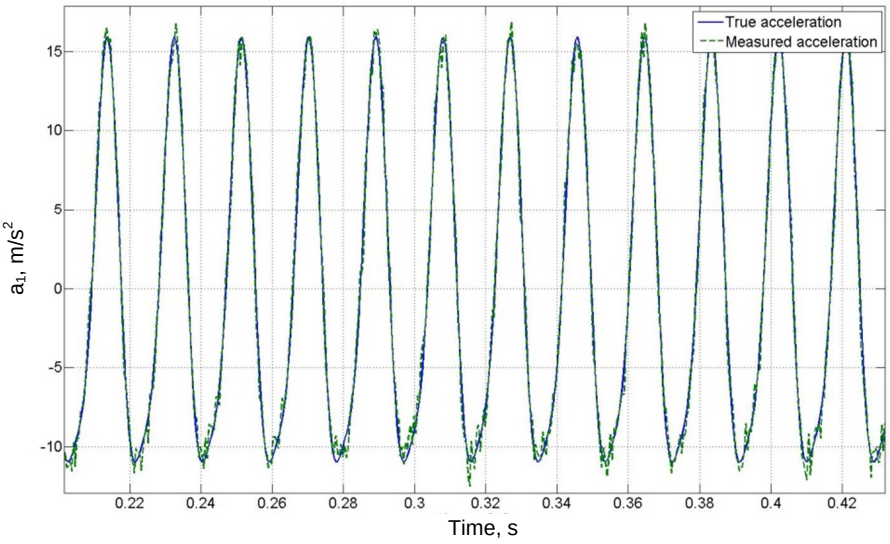

Fig. 5. Sample acceleration signal without and with random error

The numerical tests were conducted for various levels of errors in force and acceleration measurement as well as for various tooth passing frequencies (various spindle rotational speeds). Six levels of standard deviations of the force measurement error were assumed $\sigma_{force} = 0, 5, 10, 15, 20, 25$ N as well as 9 levels of standard deviations of the acceleration measurement error $\sigma_{acc} = 0, 0.2, 0.4, 0.6, 0.8, 1.0, 1.2, 1.4, 1.6$ m/s^2 and the following 12 values of tooth passing frequencies $f_t = 53, 58, 63, 68, 73, 78, 83, 88, 93, 98, 103, 108$ Hz. Thus, 648 variants were considered. Each variant was performed 10 times which allowed determination of the root mean square error (RMSE).

In many cases, the coefficients obtained with the use of the TLS method assume negative values, which is of no physical meaning. Therefore, the results obtained with this method were only presented in Fig. 6.

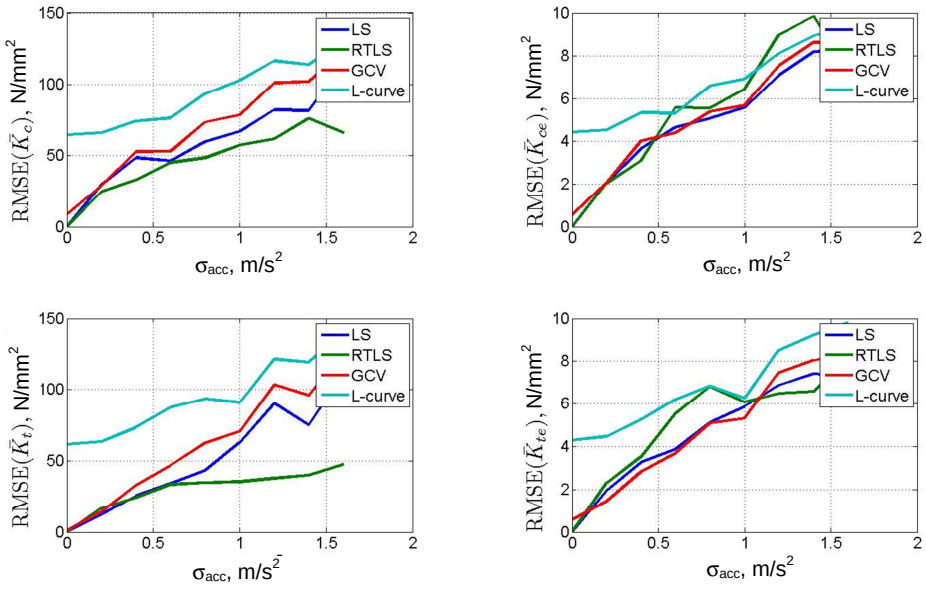

Fig. 6. Influence of acceleration measurements error on the estimation accuracy

Figure 6 presents values of the root mean square error of the determined coefficients obtained for various levels of error in acceleration measurement and for the ideal force measurement ($\sigma_{force} = 0$ [N]). It might be concluded that the use of the proposed regularization facilitates an improvement in the estimation accuracy. The root mean square error in the estimation of coefficients K_c and K_t obtained with the proposed RTLS method does not exceed 10% of the added

values of these coefficients within the range up to $\sigma_{acc} = 1.0$ [m/s^2]. Tikhonov regularization combined with L-curve method were found to be the least accurate, giving less accurate results than GCV. This could be expected due to the low dimension of the FRF matrix [10]. Slightly better results are obtained using Tikhonov regularization and GCV method but it still performs worse than LS method without regularization. It should be noted that in the considered problem we deal with low condition numbers where the unregularized solution is preferable [11]. Similar observations can be made from the Fig. 7 - Fig. 9 where the estimators accuracy is expressed as the function of force measurement error, condition number and transfer matrix error respectively.

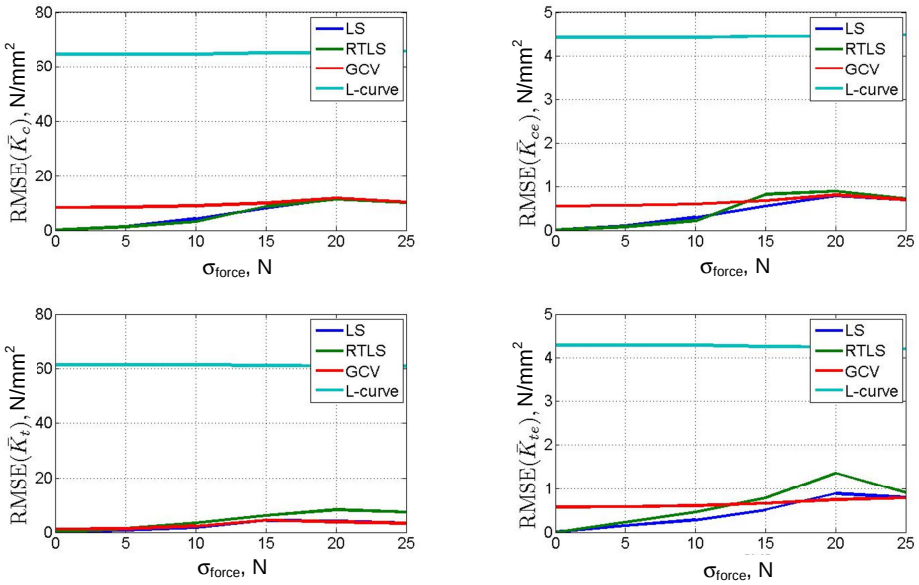

Fig. 7. Influence of force measurements error on the estimation accuracy

Figure 7 shows the influence of the error in force measurement during the impulse test on the mean square error with the assumed ideal acceleration measurement ($\sigma_{acc} = 0$ [m/s^2]). The force measurement error on the estimation accuracy was observed to be of negligible influence. Within the range of the tested values of the standard deviations in the force measurement error, the values of the root mean square error are one order lower than for the analysed standard deviations in the acceleration signal measurement error.

Figure 8 presents the influence of the matrix $\mathbf{G}^{1-2}$ conditioning on the accuracy of the obtained estimates. The course of the curves specifying this dependence is similar in terms of quality for all the compared methods.

Nevertheless, there is no significant influence of the matrix $\mathbf{G}^{1-2}$ conditioning on the estimation accuracy: the estimation errors are not proportional to the conditional numbers. The conclusion, however, is not of general character, but is only related to the conditioning range of the FRF function matrices which were present in the conducted numerical experiment. Nonetheless, it might be suggested that in similar tasks of inverse identification, the conditioning of the FRF matrix is not a factor which decides the estimation accuracy. Therefore, the use of methods which improve the conditioning of the FRF matrix (e.g. Truncated Singular Value Decomposition) are not expected to bring the expected results.

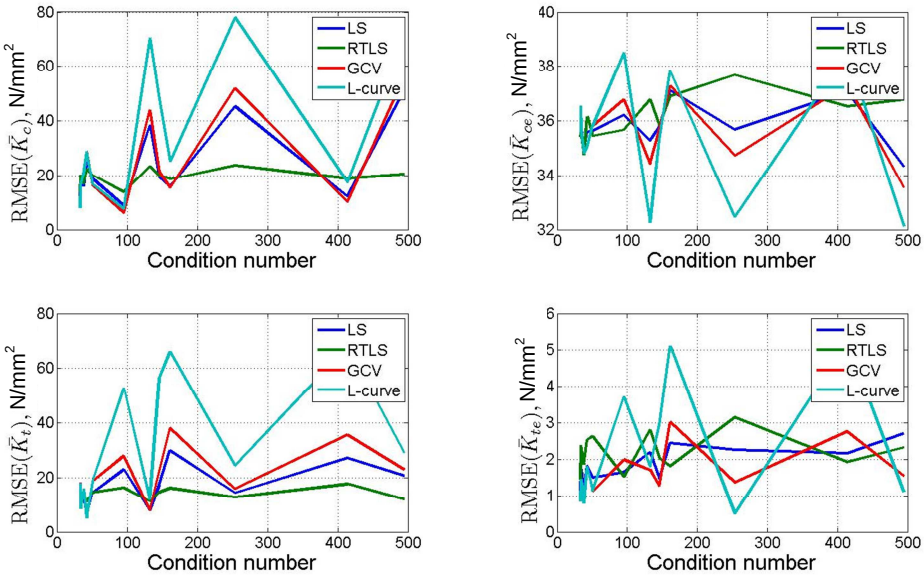

Fig. 8. Influence of the FRF matrix conditioning on the estimation accuracy

Figure 9 illustrates the influence of the errors in the determination of the FRF matrix $\mathbf{G}^{1-2}$ on the estimation accuracy. The error was determined as:

$$\varepsilon_G = \frac{\left\| \mathbf{G}^{1-2} - \mathbf{G}^{1-2}_{\text{exp}} \right\|}{\left\| \mathbf{G}^{1-2} \right\|} \tag{24}$$

where $\mathbf{G}^{1-2}$ and $\mathbf{G}^{1-2}_{\text{exp}}$ stand respectively for the theoretical (precise) and the experimental (error burdened) FRF matrix.

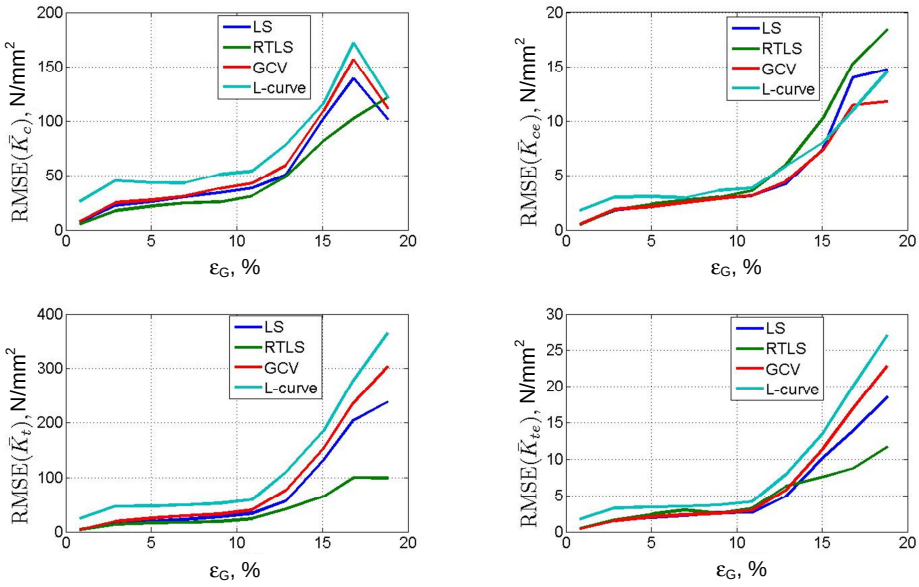

Fig. 9. Influence of the FRF matrix error on the estimation accuracy

The coefficient estimation of the machine cutting process model with the use of the RTLS method is much more resistant to the FRF matrix error than the LS method and Tikhonov regularization. The root mean square errors of the estimators of the coefficients K_c and K_t are characterised by a similar error functions. However, for the RTLS method, within the range up to the value of ε_G=15%, the root mean square error was found to not exceed 10% of the precise value of coefficients K_c and K_t.

6. Conclusions

The article presents a method for identifying the coefficients of the mechanistic cutting forces model without the necessity for direct measurement of the cutting force. These forces are identified based on the acceleration signals measured during machine cutting coupled with the use of the frequency response function matrix. An original regularization method was proposed based on the relationship between the identified harmonic components of the cutting forces. The dependence was obtained based on the mechanistic model of the cutting force. As a result of the conducted numerical tests, it was concluded that the estimation of the coefficients of the mechanistic model with the use of the TLS method extended with the proposed regularization technique is more accurate

than the TLS and LS methods. Additionally the Tikhonov regularization technique combined with L-curve and GCV were tested. It was found that the application of Tikhonov regularization gives less accurate results than the unregularized (LS) solution. This is attributed to the low condition number of the applied FRF matrix. In addition, the analysis showed that the FRF matrix errors have more of a significant influence on the estimation accuracy than matrix conditioning.

Acknowledgements

The authors would like to thank the Ministry of Science and Higher Education of the Republic of Poland for financially supporting this research under Contract No. N R03-0031-04.

References

[1] J. GRADIŠEK, M. KALVERAM, K. WEINERT: Mechanistic identification of specific force coefficients for a general end mill. *Journal of Machine Tools and Manufacture*, **44** (2004), 401–414.
[2] S. JAYARAM, S.G. KAPOOR, R.E DEVOR: Estimation of the specific cutting pressures for mechanistic cutting force model. *Journal of Machine Tools and Manufacture*, **41** (2001), 265-281.
[3] J.J. JUNZ WANG AND C.M. ZHENG: An analytical force model with shearing and ploughing mechanisms for end milling. *Journal of Machine Tools Manufacture*, **42** (2002), 761-771.
[4] B. POWAŁKA, M. PAJOR, S. BERCZYŃSKI: Identification of nonlinear cutting process model in turning. *Advances in Manufacturing Science and Technology*, **33** (2009) 3, 17-25.
[5] M. HOFFMAN, B. POWAŁKA, S. BERCZYŃSKI, M. PAJOR: Identification of cutting forces in frequency domain for milling. *Advances in Manufacturing Science and Technology*, **34** (2010) 1, 5-20.
[6] B. POWAŁKA, J. DHUPIA, G. ULSOY, R. KATZ: Identification of Machining force model parameters from acceleration measurements. *Journal for Manufacturing Research*, **3** (2008), 265-284.
[7] Y. ALTINTAS, E. BUDAK: Analytical prediction of stability lobes in milling. *Annals of the CIRP*, **44** (1995), 357-362.
[8] G.H. GOLUB, M. HEATH, G. WAHBA: Generalized cross-validation as a method for choosing a good ridge parameter. *Technometrics*, **21** (1979)2, 215-223.
[9] P.C. HANSEN: Analysis of discrete ill-posed problems by means of the L-curve. *SIAM* Rev., **34** (1992), 561-580.
[10] H.R. BUSBY, D.M. TRUJILLO: Optimal regularization of an inverse dynamics problem. *Computers and Structures*, **63** (1997), 243-248.
[11] H.G. CHOI, A.N. THITE, D.J. THOMPSON: Comparison of methods for parameter selection in Tikhonov regularization with application to inverse force determination. *Journal of Sound and Vibration*, **304** (2007), 894-917.

Received in January 2012